УДК 691.32 DOI: 10.33979/2073-7416-2020-90-4-32-45

G.A. MOISEENKO[1]
[1]Research Institute of Building Physics RAABS, Moscow, Russia

METHOD FOR CONSTRUCTION OF ISOCHRONDIAGRAMS OF HIGH-STRENGTH STEEL FIBER CONCRETE AND ITS MATRIX

Abstract. *High-strength steel fiber concrete, made on the basis of fine-grained high-strength concrete, is a quite promising building material, in particular, for the construction of high-rise buildings and structures of increased massiveness. The introduction of steel fiber into the concrete matrix can significantly reduce the influence of such shortcomings of fine-grained concrete as increased fragility and explosive nature of fracture, and also positively affects the tensile properties of concrete. However, the widespread use of high-strength steel fiber concrete is currently limited, among other things, by the lack of an experimentally relied normative framework for this material. The proposed article aims to bridge this gap. Modern engineering trends are aimed at introducing into practice diagram methods of calculation based on real diagrams of material deformation under load. This article describes the technique of constructing isochron diagrams for fine-grained high-strength concrete and steel fiber concrete with disperse reinforcement in the amount of 1.5% by weight, made from Russian-made components. Isochron diagrams allow you to calculate the deformation of the material depending on the level of load at any time, including during prolonged loading. There have been made changes to the existing methodology, allowing to take into account the nonlinearity of both current and ultimate creep characteristics depending on the level of loading. The proposed theoretical dependences give good convergence with the experimental data.*

Keywords: *high-strength steel fiber concrete, fine-grained high-strength concrete, diagram method of calculation, isochron diagrams, creep of concrete.*

Г.А. МОИСЕЕНКО[1]
[1]Научно-исследовательский институт строительной физики РААБС, г. Москва, Россия

МЕТОД ПОСТРОЕНИЯ ДИАГРАММ-ИЗОХРОН ВЫСОКОПРОЧНОГО СТАЛЕФИБРОБЕТОНА И ЕГО МАТРИЦЫ

Аннотация. *Высокопрочный сталефибробетон, изготовленный на основе мелкозернистого высокопрочного бетона, является весьма перспективным строительным материалом, в частности, для строительства высотных зданий и сооружений повышенной массивности. Введение стальной фибры в матрицу бетона позволяет значительно снизить влияние таких недостатков мелкозернистого бетона, как повышенная хрупкость и взрывной характер разрушения, а также положительно влияет на свойства бетона при растяжении. Однако широкое использование высокопрочного сталефибробетона в настоящее время ограничено, среди прочего, отсутствием экспериментально обоснованной нормативной базы для этого материала. Предлагаемая статья призвана восполнить этот пробел. Современные направления техники направлены на внедрение в практику диаграммных методов расчета на основе реальных диаграмм деформирования материала под нагрузкой. В статье описана методика построения изохронных диаграмм для мелкозернистого высокопрочного бетона и фибробетона с дисперсным армированием в количестве 1,5% по массе, изготовленных из комплектующих российского производства. Изохронные диаграммы позволяют рассчитать деформацию материала в зависимости от уровня нагрузки в любой момент, в том числе при длительном нагружении. Внесены изменения в существующую методику, позволяющие учитывать нелинейность как текущих, так и предельных характеристик ползучести в зависимости от уровня нагрузки. Предложенные теоретические зависимости хорошо сходятся с экспериментальными данными.*

Ключевые слова: *высокопрочный сталефибробетон, мелкозернистый высокопрочный бетон, диаграммный метод расчета, изохронные диаграммы, ползучесть бетона.*

1. Introduction

The rapid development of the construction industry, as well as modern trends in construction, aimed at the construction of unique, including high-rise and super-tall structures, require the development and improvement of the materials used. High-strength fine-grained concrete (HSFGC) opens up broad prospects for work in this direction. However, its main drawbacks, such as increased fragility and explosive nature of destruction, limit itsapplication area.One of the solutions to this problem is the introduction of dispersed reinforcement into concrete. In this regard, high-strength steel fiber concrete (HSSFC) is of increasing interest. Its widespread use is constrained by the relatively high cost of steel fiber and the lack of a regulatory framework necessary for the design based on experimental studies of its properties. The latter determines the relevance of the proposed study.

The study of the behavior of varieties of HSSFC under various influences is carried out both in Russia [1, 2, 3, 4, 5, 6] andabroad [7, 8, 9, 10]. In our country, studies have been conducted of steel fiber reinforced concrete with a high fiber content, obtained according to the original technology from highly mobile and self-compacting mixtures of Russian production [11, 12, 13]. This article describes a study of a similar composition with a minimum effective percentage of dispersed reinforcement.

According to [14], in modern design practice, diagram methods of calculation are increasingly used, which are based on real diagrams of material deformation under load. In this regard, for new types of investigated high-strength concrete, the development of a technique for constructing isochron diagrams, which make it possible to determine deformations depending on the load level at any moment of loading, seems to be very relevant.

2. Methods

For constructing isochron diagrams of the studied compositions, the results of extensive experimental studies [15] were used, covering a wide range of physicomechanical and rheological properties of high-strength steel fiber concrete in comparison with an unreinforced matrix, fine-grained high-strength concrete. The composition of the matrix was assigned in accordance with [16, 17, 18]. It was adoptedthe following:

- Portland cement grade ПЦ 500 ДОН 900 кг/м^3;
- superplasticizer МБЗ-50К 360 кг/м^3;
- sand with particle size $M_к$ = 2,5 860 кг/м^3;
- water 190 кг/м^3.

To evaluate the effect of steel fiber on creep and shrinkage deformations, two series of prism samples 7x7x28 (cm) in size were used. The first series was made without steel fiber, and in the second series direct brass high-strength fiber with Ø 0.3 mm and a length of 13 mm in the amount of 1.5% of the volume was introduced. According to the results of [15], such a percentage of fiber content is a kind of minimum efficiency threshold for a given type of concrete. Concrete compositions can be attributed to self-compacting, since the cone spread is more than 60 cm.

After formwork removal carried out in two days, the samples were placed in a chamber of normal hardening. According to the research program, the loading of samples was carried out at the age of 7, 28 and 100 days for both series. Before loading started, samples were removed from the chamber at that time and were isolated with two layers of paraffin to maintain the temperature and humidity conditions inside the sample. Further, they were mounted frames for the installation of instruments for measuring longitudinal and transverse strains.To measure longitudinal and transverse strains, dial gauges with a division value of 0.01 and 0.001 mm were used.

Before loading on a long-term exposure, short-term tests were conducted to determine the prism strength and other physical and mechanical characteristics for a given age.

The average level of prism strength was used to determine the relative level of $0.3R_b$, $0.6R_b$ and $0.8R_b$ for long-term tests.

Let us dwell on the description of longitudinal deformations.

3. Results and discussion

Table 1 shows the values of longitudinal creep deformations of samples ε_{b1}^{c} measured at 180 days of age, instantly elastic deformations ε_{b1}^{e} measured at the beginning of loading, as well as the values of total deformations ($\varepsilon_{b1}^{e}+\varepsilon_{b1}^{c}$) for samples loading at 7, 28 and 100 days.

Table 1 - The results of experimental studies

	Age, days	$\frac{\sigma_b}{R_b}$	$\varepsilon_{b1}^{e}\times10^5$	$\varepsilon_{b1}^{c}\times10^5$	$(\varepsilon_{b1}^{e}+\varepsilon_{b1}^{c})\times10^5$
HSFGC	7	0.3	77.00	91.61	168.61
		0.6	156.91	267.24	424.15
	28	0.3	84.92	78.20	163.12
		0.6	180.16	212.22	392.38
		0.8	221.50	285.13	506.63
	100	0.3	104.49	72.25	176.74
		0.6	171.24	163.49	334.73
HSSFC	7	0.3	70.67	73.42	144.09
		0.6	139.83	165.42	305.25
	28	0.3	76.67	59.17	135.84
		0.6	166.01	165.77	331.78
		0.8	204.58	245.31	449.89
	100	0.3	76.09	50.26	126.35
		0.6	165.33	122.00	287.33

The experimental studies performed correspond to the rigid loading regime according to [14]. In this mode, the load applied to the test samples is brought to the design level in a short time (within one hour) and then kept constant for a long time.

To construct isochron diagrams, we apply the traditional theoretical approach described in [19] and developed in [14], and we will correct it as applied to the materials under study on the base of experimental data.

First of all, it is necessary to determine the vertices of the isochron diagrams by plotting the long-term resistance curves of concrete. For each investigated moment of loading time, the load level will be determined from the value of long-term resistance at this point. Studies by various authors [20-22] suggest that during prolonged loading of concrete with high level compressive stresses, its strength decreases by an average of 10-25%. In the case of a rigid loading regime, the long-term resistance curve has a section of a sharp decrease in strength and then stabilizes. When constructing the curve, the age of the concrete at loading t_0 and the loading time $t - t_0$ are taken into account. For this, the following dependence is used:

$$R_{b,ser}(t,t_0)=R_{b,ser}(t_0)\left\{[0.95-1.57\cdot10^{-2}\ln(t-t_0)]\gamma_t+\frac{\bar{\gamma}_{b2}(1-\gamma_t)}{1-(1-\bar{\gamma}_{b2})e^{-4\gamma_1(t-t_0)}}\right\}, \quad (1)$$

where $\gamma_t = 1$ for rigid loading regime;

γ_{b2} is the coefficient taking into account concrete age and the effect of hardening conditions on long-term resistance, under normal hardening conditions is calculated by the formula

$$\gamma_{b2}=0.85+1.44e^{-0.12t_0};$$

$R_{b,ser}(t_0)$ is initial compressive strength depending on load age.

According to [14], by the time moment *t*, the deformations of the sample under the rigid loading regime are composed of the instantly elastic component and creep deformations. In general terms, this can be represented by the following dependence (2):

$$\varepsilon_b(t)=\sigma_b(t_0)\left[\frac{1}{E_b(t_0)\nu_b}+f_C C(t,t_0)\right]=\frac{\sigma_b(t_0)}{E_b(t_0)}\left[\frac{1}{\nu_b}+f_C\varphi(t,t_0)\right], \quad (2)$$

where$E_b(t_0)$ is modulus of elasticity of concrete corresponding to the age of loading t_0; $\nu_b$is the coefficient of change of the secant modulus during short-term compression; $C(t,t_0)$ islinear creep measure; f_C is nonlinearity function; $\varphi(t,t_0)$is creep characteristic, while

$$\varphi(t,t_0) = E_b(t_0)C(t,t_0). \quad (3)$$

Anoverall measure of linear and nonlinear creep is presented in the form (4):

$$C(t,t_0,\eta) = f_C C(t,t_0) = \frac{f_C\varphi(t,t_0)}{E_b(t_0)}. \quad (4)$$

The creep characteristic is determined by the expression

$$\varphi(t,t_0) = \varphi f(t-t_0), \quad (5)$$

where$\varphi = \varphi(\infty,t_0)$is ultimate characteristic of linear creep, the expression for which is constructed as follows:

$$\varphi = \varphi^N \xi_1 \xi_2 \Omega(t_0) \quad (6)$$

The functions $f(t-t_0)$ and $\Omega(t_0)$, respectively, taking into account the development of creep deformations in time and the influence of the loading age on the creep characteristic, are calculated by the formulas:

$$f(t-t_0) = 1 - De^{-\alpha(t-t_0)} - Be^{-\gamma_1(t-t_0)},$$

$$\Omega(t_0) = 0.5 + de^{-2\gamma_1 t_0};$$

a description of the parameters included in these relationships and their adjustment in relation to the HSFGC and HSSFC of the type under study are described in [19].

The coefficients ξ_1 and ξ_2 are introduced to take into account, respectively, the influence of humidity of the medium and the conditions of moisture exchange with the medium and are assigned in accordance with [14].

For the conditions in which our experiments were conducted, these coefficients are accepted as follows: ξ_1 =0.47, $\xi_2 = 0.52$.

The parameter φ^N represents the limiting function for concretes under reference conditions and depends mainly on the type of concrete. For the materials under study, it was found based on a comparison of theoretical and experimental data and amounted to:

- $\varphi^N = 4.5$ for HSFGC;
- $\varphi^N = 3.6$ for HSSFC.

Expressions (5) and (6) can be brought into correspondence with the classical formula of the experimental approach to the description of creep measures:

$$C(t,t_0) = C(\infty,28)\Omega(t_0)f(t-t_0),$$

whence, taking into account (3), we obtain

$$C(\infty,28) = \frac{\varphi^N \xi_1 \xi_2}{E_b(t_0)}.$$

The nonlinearity function is traditionally constructed as

$$f_C = 1 + \upsilon_c \eta^4(t_0).$$

For isochron diagrams, it is necessary to go to the current stress level; presenting it in the form

$$\eta(t,t_0) = \eta(t_0)\tilde{\gamma}_{b2},$$

where $\tilde{\gamma}_{b2} = \frac{R_b(t,t_0)}{R_b(t_0)}$, we get

$$f_C = 1 + \upsilon_c \tilde{\gamma}_{b2}{}^4 \eta^4(t,t_0).$$

For practical construction of isochron diagrams at any time *t*, the expression for determining the deformations of the sample is presented by analogy with the case of short-term compression, but the parameters included in it are calculated for the current loading moment $t - t_0$:

$$\varepsilon_b(t) = \frac{\sigma_b(t,t_0)}{E_b(t,t_0)\nu_b(t,t_0)}, \quad (7)$$

where the level of loading $\eta(t,t_0)=\frac{\sigma_b(t,t_0)}{R_b(t,t_0)}$; the values of the coefficient of change of the secant module can be calculated by the formulas:

$$\nu_b(t,t_0)=\hat{\nu}_b(t,t_0)+[\nu_0(t,t_0)-\hat{\nu}_b(t,t_0)]\sqrt{1-\omega\eta(t,t_0)-(1-\omega)\eta^2(t,t_0)}, \quad (8)$$

$$\omega=2-2.5\hat{\nu}_b(t,t_0).$$

The expressions for the boundary values at the beginning and at the top of the diagram are as follows. Equating the deformation values calculated by (3) and (7), we obtain

$$\nu_b(t,t_0)=\frac{\nu_b}{1+\nu_b f_C\varphi(t,t_0)} \quad (9)$$

Given that at the beginning of the diagram $\nu_b=1$, $f_C=1$; at the top of thediagram $\nu_b=\hat{\nu}_b$, $f_C=1+\upsilon_c\tilde{\gamma}_{b2}{}^4$, for the ascending branch, the boundary values are

$$\nu_0(t,t_0)=\frac{1}{1+\varphi(t,t_0)} \quad (10)$$

$$\hat{\nu}_b(t,t_0)=\frac{\hat{\nu}_b}{1+\hat{\nu}_b\left(1+\upsilon_c\tilde{\gamma}_{b2}{}^4\right)\varphi(t,t_0)}, \quad (11)$$

where$\hat{\nu}_b$is the coefficient of change of the secant modulus during short-term compression calculated for the studied compositions according to the method described in [24].

It should be noted that expression (9) can be used both for directly calculating the coefficient of change of the secant modulus at the current moment of time and for determining boundary values, and the overall expression for the current value can be taken from (8). We use the second approach, which gives according to [14] a more accurate agreement with experimental data.

The elastic modulus $E_b(t,t_0)$ included in expression (7) can be taken in different ways: as the initial module for a given loading age $E_b(t_0)$, as the current value for time *t*, as an average module in the time interval $t-t_0$. For the rigid loading regime, we will take the first version of the calculation of the elastic modulus.

The construction of the theoretical isochron under infinitely long loading (with$t\to\infty$) is also performed according to the presented dependences with the difference that in formulas (9) and (10) the current creep characteristic $\varphi(t,t_0)$ is replaced by the ultimateφ. When calculating the long-term resistance at infinity by formula (1), the interval $t-t_0$ is taken to be 365 days.

When constructing the isochron diagrams of HSFGC and HSSFC and comparing the results with experimental data, it became necessary to correct the described calculation algorithm. The following additions and changes are proposed.

1. Taking into account that the function$f(t-t_0)$, which takes into account the development of creep in time, gives large errors at the initial stages of loading, it is necessary to introduce the factor $\Delta(t,t_0)$, which takes into account the influence of fast-flowing creep. Traditionally, it is used under soft loading regimes, however, a comparison with experimental data indicates the need for its application for rigid loading regimes. At $t-t_0\le 1$ day, we multiply the function $f(t-t_0)$ by the expression

$$\Delta(t,t_0)=\sqrt{1+0{,}314\ln(t-t_0)},$$

then formula (5) takes the form

$$\varphi(t,t_0)=\varphi f(t-t_0)\Delta(t,t_0).$$

When $t-t_0>1$ day, the multiplier $\Delta(t,t_0)=1$.

2. It is proposed to modify the structure of the creep characteristic φ, converting it from linear to overall using the nonlinearity function. We represent (7) in the form:

$$\varphi=\varphi^N\xi_1\xi_2\Omega(t_0)\,f_C$$

Such a record makes it possible to lay nonlinearity depending on the level of acting stresses in the creep characteristic, i.e., (3) takes the form

$$C(t,t_0,\eta)=\frac{\varphi(t,t_0)}{E_b(t_0)} \quad (12)$$

In this case, the ultimate measure of creep at a loading age of 28 days, as a comparison of theoretical and experimental data shows, with an acceptable degree of error can also be calculated by the formula

$$C(\infty, 28) = \frac{\varphi^N \xi_1 \xi_2}{E_b(t_0)} f_C \quad (13)$$

The nonlinearity function also needs to be adjusted based on agreement with the experimental data. We accept f_C as

$$f_C = 1 + \upsilon_c \tilde{\gamma}_{b2}{}^2 \eta^2(t, t_0)$$

When changing the age of loading of concrete, the nonlinearity function, while maintaining the general structure, changes its "amplitude". This can be taken into account by the coefficient υ_c, which depends on the type of concrete and the age of loading. The selected values for the studied materials are shown in table 2.

Table 2 - Coefficients υ_c for HSFGC and HSSFC depending on age of loading

Loading aget_0	HSFGC	HSSFC
7 days	0.2	0.08
28 days	0.9	0.9
100 days	1.9	1.4

The proposed changes make it possible to uniformly describe the nonlinearity of the creep characteristics, as well as to verify the experimental creep measures obtained. It should be noted that at high load levels close to 1, the proposed designs of creep measures and nonlinearity functions require refinement and additional studies.

When using the proposed expressions of creep characteristics, formulas (10), (11) to calculate the boundary values of the coefficient of change of the secant module take the form:

$$\nu_0(t, t_0) = \frac{1}{1+\varphi_0(t,t_0)}$$

$$\hat{\nu}_b(t, t_0) = \frac{\hat{\nu}_b}{1+\hat{\nu}_b\hat{\varphi}(t,t_0)},$$

where $\varphi_0(t, t_0)$ and $\hat{\varphi}(t, t_0)$ are accordingly the creep characteristics at the beginning of the diagram for $\eta(t, t_0) = 0$ and at the top of the diagram for $\eta(t, t_0) = 1$.

The results of constructing theoretical isochron diagrams with the indicated changes must be verified by comparison with experimental data.

The main check will be the superposition of isochron diagrams for time instants of 0.05 day and 180 days on experimental diagrams constructed according to the data in Table 1. A comparison of the diagrams is shown in figure 1 - 6. For concrete loaded in 28 days, we also give diagrams of short-term compression for comparison with isochrone of 0.05 day. The technique for obtaining short-term compression diagrams for the concrete under study is described in detail in [24].

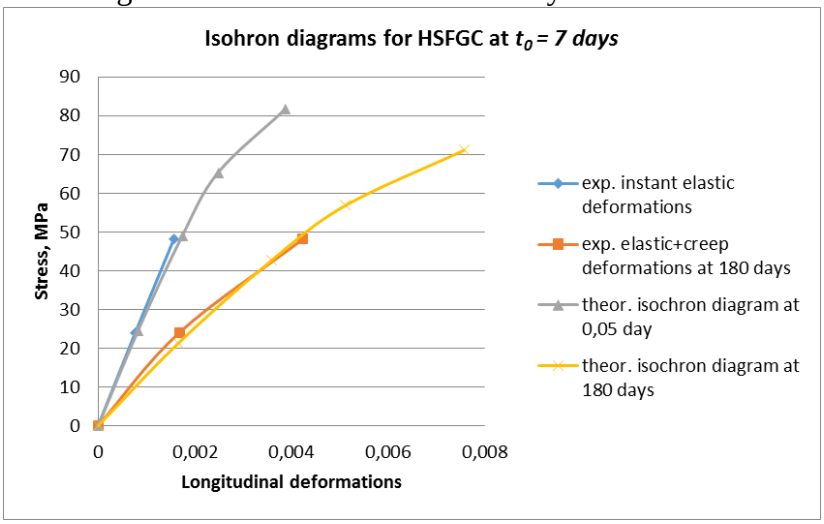

Figure 1 - Comparison of theoretical and experimental isochron diagrams for the HSFGC loaded in 7 days

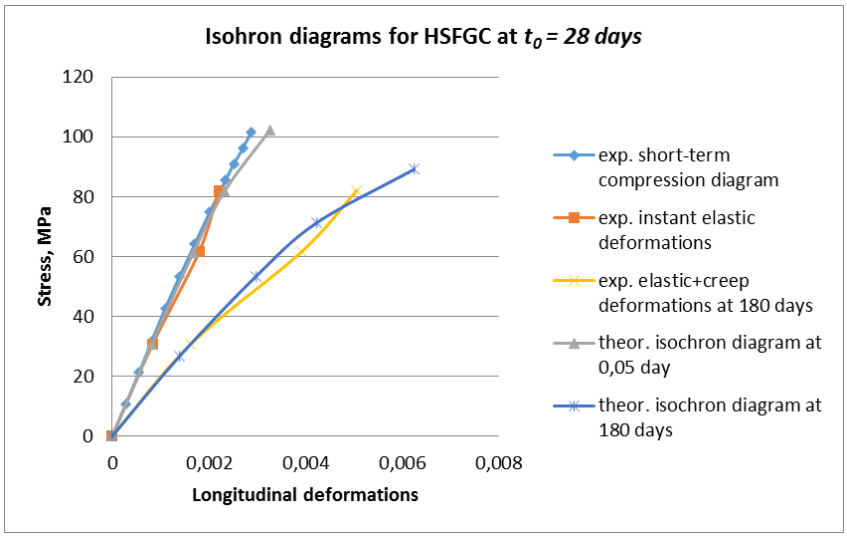

Figure 2 - Comparison of theoretical and experimental isochron diagrams for the HSFGC loaded in 28 days

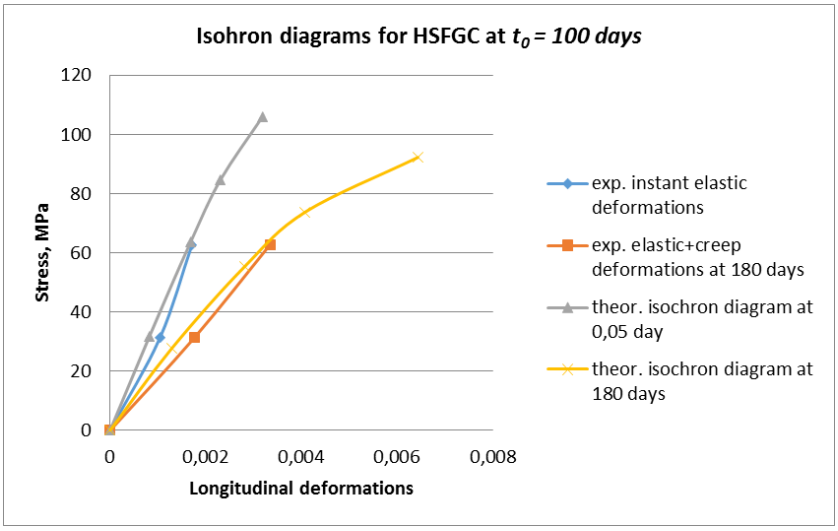

Figure 3 - Comparison of theoretical and experimental isochron diagrams for the HSFGC loaded in 100 days

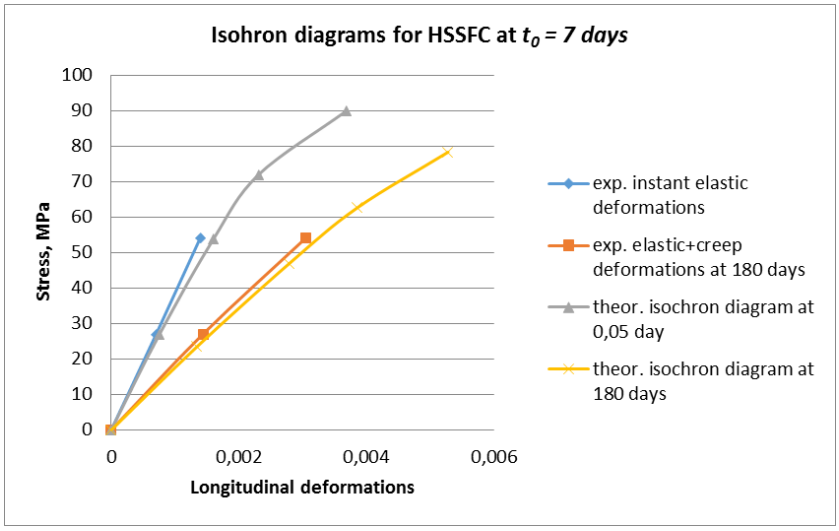

Figure 4 - Comparison of theoretical and experimental isochron diagrams for the HSSFC loaded in 7 days

We also compare the ultimate creep measures calculated experimentally by the technique of [25] with the theoretical data by formula (13). The comparison results are shown in figure 7 - 8.

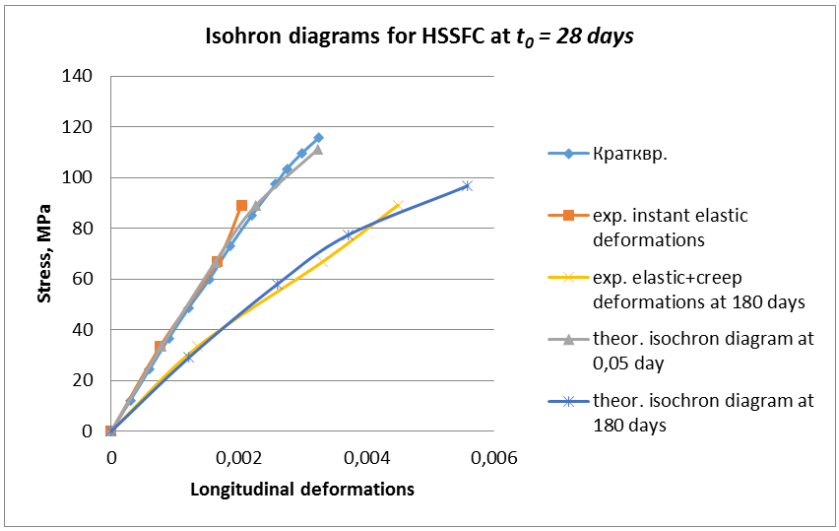

Figure 5 - Comparison of theoretical and experimental isochron diagrams for the HSSFC loaded in 28 days

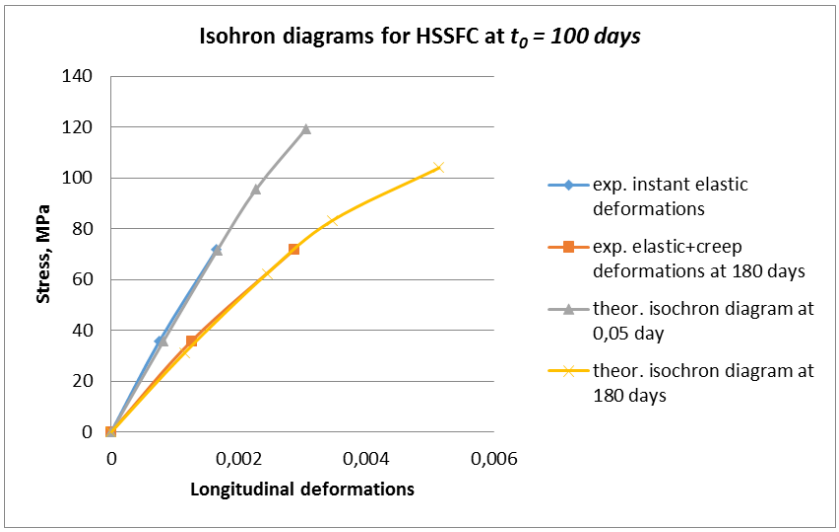

Figure 6 - Comparison of theoretical and experimental isochron diagrams for the HSSFC loaded in 100 days

Figure 7 - Comparison of theoretical and experimental ultimate creep measures for the HSFGC loaded in 28 days

Figure8 - Comparison of theoretical and experimental ultimate creep measures for the HSSFC loaded in 28 days

Finally, we compare the theoretical curves of the current overall creep measures obtained using formula (12) with the experimental ones. The results are presented in figure 9-14.

Experimental charts of overall creep measures were obtained on the basis of the curves of relative creep deformations $\varepsilon_{\text{br}}(t,t_0)$ constructed when measuring creep deformations in a study [15]:

$$C(\eta,\text{t},t_0)=\varepsilon_{br}(t,t_0)/\sigma_b(t_0),$$

where $\sigma_b(t_0)$ is stresses equal $0.3\text{R}_\text{b}(t_0)$, $0.6\text{R}_\text{b}(t_0)$, $0.8\text{R}_\text{b}(t_0)$, which were applied to samples at the age of $t_0=7\ days$, $t_0=28\ days$, $t_0=100\ days$; t is the current time of the sample under load ($\text{t}\geq t_0$).

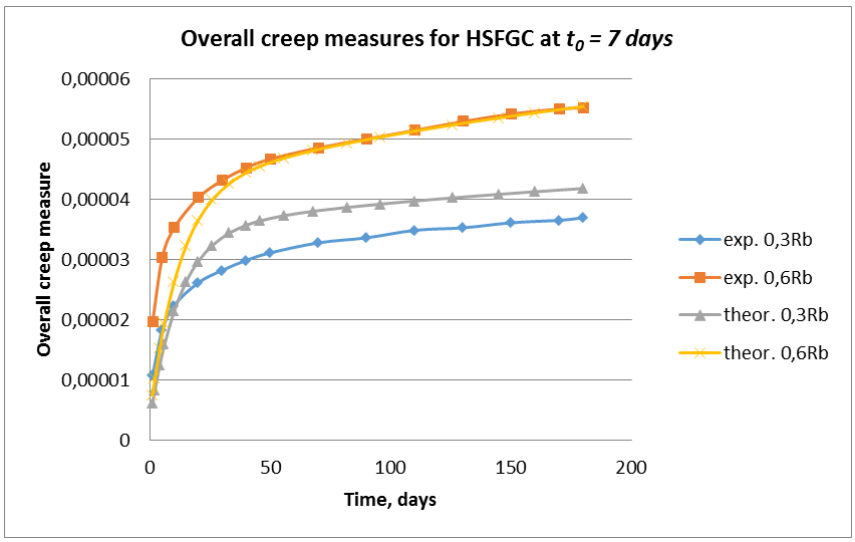

Figure 9 - Comparison of theoretical and experimental current creep measures for the HSFGC loaded in 7 days

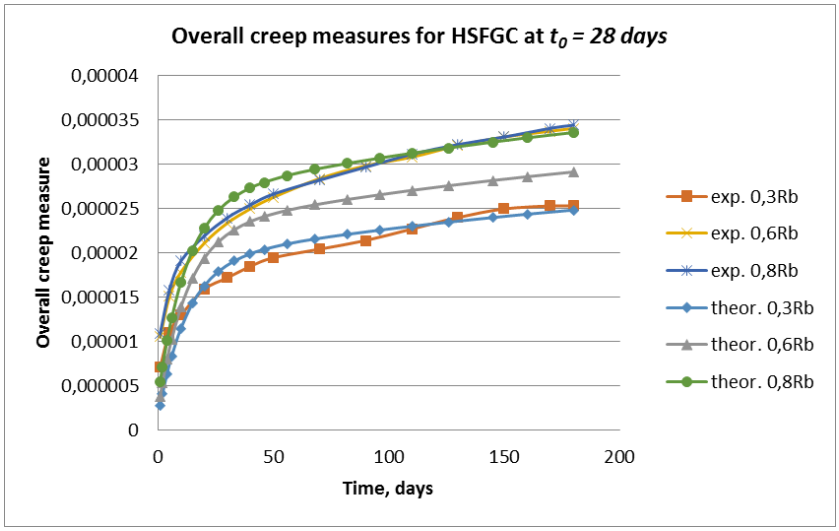

Figure 10 - Comparison of theoretical and experimental current creep measures for the HSFGC loaded in 28 days

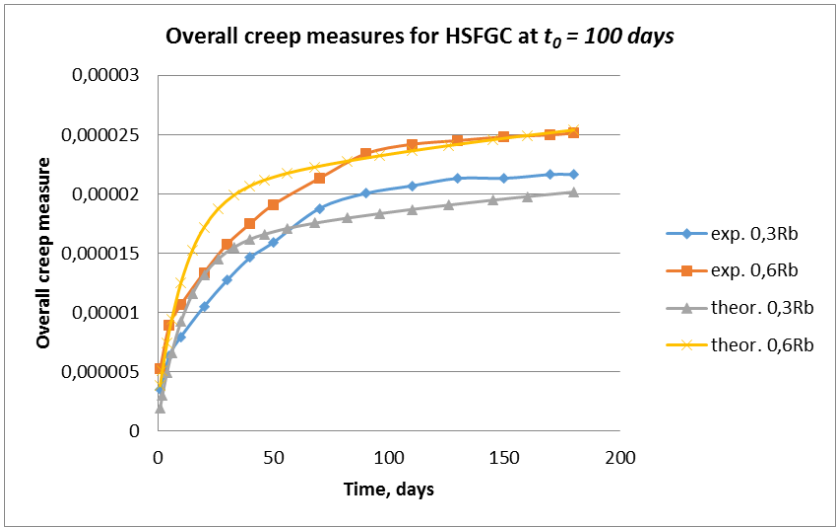

Figure11 - Comparison of theoretical and experimental current creep measures for the HSFGC loaded in 100 days

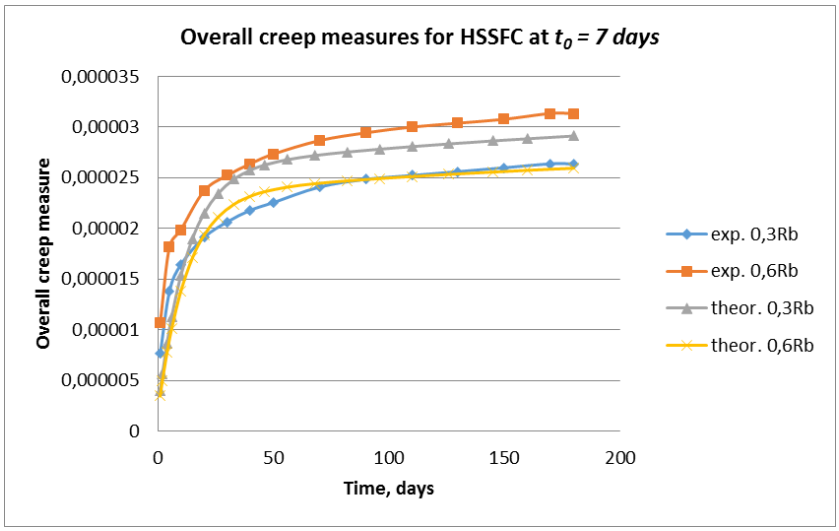

Figure 12 - Comparison of theoretical and experimental current creep measures for the HSSFC loaded in 7 days

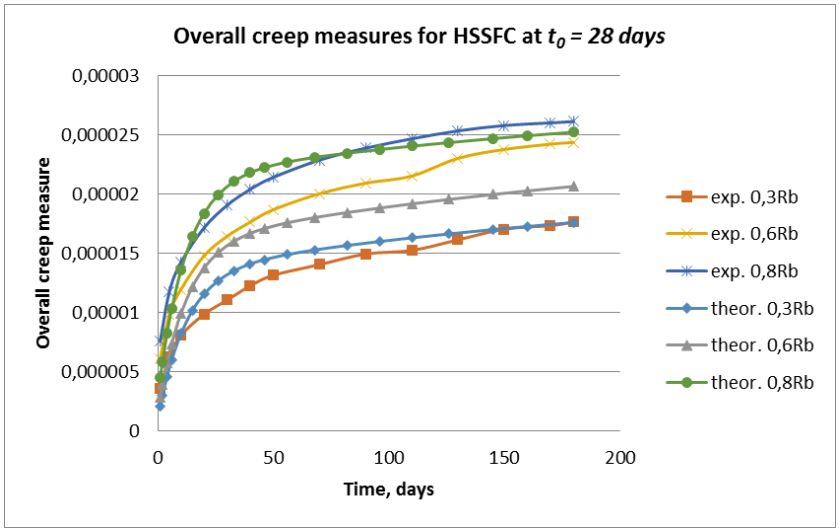

Figure 13 - Comparison of theoretical and experimental current creep measures for the HSSFC loaded in 28 days

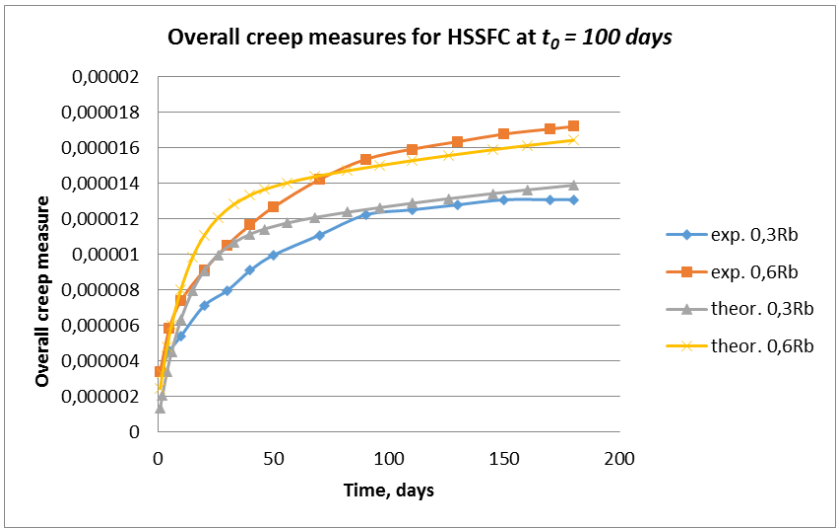

Figure 14 - Comparison of theoretical and experimental current creep measures for the HSSFC loaded in 7 days

4. Conclusions

Based on the results of the study, we can draw the following conclusions:

- A methodology has been developed for constructing the full range of isochron diagrams, starting from 1 hour of loading, for a new type of HSFGC and HSSFC of different ages. Comparison of the curves obtained theoretically shows good convergence with the data of experimental studies.
- Suggestions were made to improve the existing approach to the description of creep characteristics. Modified dependencies are proposed that allow to take into account the nonlinearity of both current and limiting creep measures depending on the load level.
- The proposed methods and dependencies can be used in the design and calculation of structures basing on modern diagram methods.

REFERENCES

1. Korsun V., Vatin N., Franchi A., Korsun A., Crespi P., Mashtaler S. The Strength and Strain of High–Strength Concrete Elements withConfinementand Steel Fiber Reinforcement including the Conditions of the Effect ofElevated Temperatures. // International Scientific Conference Urban Civil Engineering and Municipal Facilities, SPbUCEME, 2015. ProcediaEngineering (SCOPUS), 2015. No. 117. P. 975 – 984.
2. Korsun V., Korsun A., Mashtaler S. Determination of the Critical Duration of the First Heating of Heavy Concrete by the Criterion of the Maximum Strength Reduction // Applied Mechanics and Materials. Trans tech Publications, Switerland. 2015. Vols. 725 – 726. Pp. 566 – 571. [Electronic resource]. URL: https://www.scientific.net/ /AMM.725–726.566
3. Mashtaler S.N., Korsun V.I. Vliyaniye kratkovremennogo nagreva na prochnost' i deformatsii vysokoprochnogo stalefibrobetona pri osevom szhatii i rastyazhenii [The influence of short-term heating on the strength and deformation of high-strength steel fiber concrete under axial compression and tension] // Collection of abstracts on the materials of the conference "Scientific and technical achievements of students, graduate students, young scientists of the construction and architectural industry." Makeyevka, 2016. P.142.
4. Barsuk N.D., Mozalevsky D.A., Kupenko I.V., Borschevsky S.V., Makarenko S.Yu., Mashtaler S.N. Laboratornyye issledovaniya fibrobetona dlya podzemnogo stroitel'stva [Laboratory studies of fiber concrete for underground construction] // Subsoil use problems: Collection of scientific papers. Part I. St. Petersburg Mining University. St. Petersburg, 2017. P. 149-153.
5. Antonie E. Naaman. Fiber Reinforced Cement and Concrete Composites. Sarasota, Techno Press 3000, 1st edition, 2018. 765 p.
6. W. Yao, L. Jie, K. Wu. Mechanical Properties of Hybrid Fiber Reinforced Concrete at Low Fiber Volume // Cement & Concrete ResearchNo. 33, 2003.P. 27-30.
7. Beddar M. Fiber reinforced concrete: past, present and future. The present and future of fiber-reinforced concrete. // Concrete and reinforced concrete - development paths. Scientific works of the 2nd All-Russian (international) conference on concrete and reinforced concrete. October 5-9, 2005, Moscow, in 5 vols. NIIZHB, 2005. Vol. 3. Section reports, section Concrete Technology, p. 228-234.
8. Abbas S., Nehdi M. L., Saleem M. A. Ultra-High Performance Concrete: Mechanical Performance, Durability, Sustainability and Implementation Challenges // International Journal of Concrete Structures and Materials. 2016. Vol. 10, No. 3. P. 271–295.
9. Gu C., Ye G., Sun W. Ultrahigh performance concrete-properties, applications and perspectives // Science China Technological Sciences. 2015. Vol. 58, Issue 4. P. 587-599.
10. Aitcin P.C. High-performance concrete, London: E&FN SPON, 1998. 591 p.
11. Mishina A.V. Issledovaniye deformatsiy polzuchesti vysokoprochnogo stalefibrobetona pri razgruzke [Investigation of creep deformations of high-strength steel fiber concrete during unloading] // Academia. Architecture and construction. 2013. No. 3.
12. Mishina A.V., Bezgodov I.M., Andrianov A.A. Prognozirovaniye predel'nykh deformatsiy polzuchesti sverkhvysokoprochnogo stalefibrobetona [Prediction of ultimate creep strains of ultrahigh-strength steel fiber concrete] // Vestnik MGSU. 2012. No. 12.
13. Karpenko N.I., Travush V.I., Kaprielov S.S., Mishina A.V., Andrianov A.A., Bezgodov I.M. Issledovaniye fiziko-mekhanicheskikh i reologicheskikh svoystv vysokoprochnogo stalefibrobetona [Investigation of the physico-mechanical and rheological properties of high-strength steel fiber concrete] // Academia. Architecture and construction. 2013. No. 1.
14. Karpenko N.I., Travush V.I. and other. Metodicheskoye posobiye «Staticheski neopredelimyye zhelezobetonnyye konstruktsii. Diagrammnyye metody avtomatizirovannogo rascheta i proyektirovaniya». [Methodological manual “Statically indefinable reinforced concrete structures. Diagrammatic methods of automated calculation and design."] //Federal Autonomous Institution “Federal Center for Standardization, Standardization and Conformity Assessment in Construction”. Moscow, 2017.
15. Karpenko N.I., Kapriyelov S.S., Petrov A.N., Bezgodov I.M., Moiseenko G.A., Stepanov M.V., Chilin I.A. Issledovaniye fiziko-mekhanicheskikh i reologicheskikh svoystv vysokoprochnykh stalefibrobetonov iz samouplotnyayushchikhsya smesey. [Investigation of the physico-mechanical and rheological properties of high-strength steel fiber reinforced concrete from self-compacting mixtures] // Fundamental, search and applied research of the RAASN on the scientific support of the development of architecture, urban planning and the construction industry of the Russian Federation in 2017. Vol. 2. Moscow, 2018. P. 237-246.
16. Kapriyelov S.S., Sheynfel'd A.V., Kardumyan G.S. Novyye modifitsirovannyye betony . [New modified concretes] // Moscow, “Printing House Paradiz” LLC. 2010. P. 258.
17. Kapriyelov S.S., Chilin I.A. Sverkhvysokoprochnyy samouplotnyayushchiysya fibrobeton dlya monolitnykh konstruktsiy [Ultra-high-strength self-compacting fiber-reinforced concrete for monolithic structures] // Construction Materials, No. 7. 2013. P. 28-30.

18. Kapriyelov S.S., Sheynfel'd A.V., Kardumyan G.S., Dondukov V.G. Modifitsirovannyye vysokoprochnyye melkozernistyye betony s uluchshennymi deformativnymi kharakteristikami [Modified high-strength fine-grained concretes with improved deformative characteristics] // Concrete and reinforced concrete. 2006. No. 2.. P. 2-7.

19. Karpenko N.I. Obshchiye modeli mekhaniki zhelezobetona. [General models of reinforced concrete mechanics] // Stroyizdat, Moscow, 1996.

20. Gvozdev A.A., Yashin A.V., Petrova K.V., Belobrov I.K., Guzeev E.A. Prochnost', strukturnyye izmeneniya i deformatsii betona. [Strength, structural changes and deformation of concrete]. Moscow: Stroyizdat, 1978.

21. Malashkin Yu.N., Bezgodov I.M. Issledovaniye dlitel'noy prochnosti i deformativnosti betona pri odno-, dvukh- i trekhosnom szhatii. [Investigation of the long-term strength and deformability of concrete under uniaxial, biaxial, and triaxial compression] // Limit states of concrete and reinforced concrete structures of power structures. Materials of conferences and meetings on hydraulic engineering. Moscow, 1987. P. 216-219.

22. Yashin A.V. Deformatsii betona pod dlitel'nym vozdeystviyem vysokikh napryazheniy i yego dlitel'noye soprotivleniye szhatiyu. [Deformation of concrete under prolonged exposure to high stresses and its long-term resistance to compression] // Features of the deformation of concrete and reinforced concrete and the use of computers to assess their impact on the behavior of structures. Moscow, Stroyizdat, 1969. P. 38-76.

23. Stepanov M.V., Moiseenko G.A. Razvitiye eksperimental'nogo podkhoda k opredeleniyu mery polzuchesti melkozernistogo vysokoprochnogo betona i stalefibrobetona pri ratsional'nom soderzhanii fibry. [Development of an experimental approach to the determination of creep measures of fine-grained high-strength concrete and steel fiber concrete with a rational fiber content] // Stroitel'stvo i rekonsruktsiya. 2018. No. 3 (77). P. 98-104.

24. Stepanov M.V., Moiseenko G.A. Diagrammy deformirovaniya melkozernistogo vysokoprochnogo betona i stalefibrobetona pri szhatii. [Deformation diagrams of fine-grained high-strength concrete and steel-fiber concrete under compression] // Stroitel'stvo i rekonsruktsiya. 2019. No.3 (83). P. 11-21.

25. GOST 24544-81 Betony. Metody opredeleniya deformatsiy usadki i polzuchesti. [Concrete. Methods for determining shrinkage and creep deformations].

СПИСОК ЛИТЕРАТУРЫ

1. Korsun V., Vatin N., Franchi A., Korsun A., Crespi P.,Mashtaler S. The Strength and Strain of High–Strength Concrete Elements withConfinementand Steel Fiber Reinforcement including the Conditions of the Effect ofElevated Temperatures. // International Scientific Conference Urban Civil Engineering andMunicipal Facilities, SPbUCEME, 2015. ProcediaEngineering, 2015. No. 117. P. 975 – 984.

2. Korsun, V., Korsun, A., Mashtaler, S. Determination of the Critical Duration of the First Heating of Heavy Concrete by the Criterion of the Maximum Strength Reduction // Applied Mechanics and Materials, 2015, Trans tech Publications, Switerland, vols. 725 – 726, p. 566 – 571. [Electronic resource]. URL: https://www.scientific.net/AMM.725–726.566

3. Машталер С.Н., Корсун В.И. Влияние кратковременного нагрева на прочность и деформации высокопрочного сталифибробетона при осевом сжатии и растяжении // Сборник тезисов по материалам конференции «Научно-технические достижения студентов, аспирантов, молодых ученых строительной и архитектурной отрасли». Макеевка, 2016. С.142.

4. Барсук Н.Д., Мозалевский Д.А., Купенко И.В., Борщевский С.В., Макаренко С.Ю., Машталер С.Н. Лабораторные исследования фибробетона для подземного строительства // Проблемы недропользования: Сборник научных трудов. Часть I. Санкт-Петербургский горный университет. Санкт-Петербург, 2017. С. 149-153.

5. AntonieE. Naaman. Fiber Reinforced Cement and Concrete Composites. Sarasota, Techno Press 3000, 1st edition, 2018. 765 p.

6. W. Yao, L. Jie, K. Wu. Mechanical Properties of Hybrid Fiber Reinforced Concrete at Low Fiber Volume // Cement & Concrete ResearchNo. 33, 2003. P. 27-30.

7. Beddar M. Fiber reinforced concrete: past, present and future. The present and future of fiber-reinforced concrete. // Concrete and reinforced concrete - development paths. Scientific works of the 2nd All-Russian (international) conference on concrete and reinforced concrete. October 5-9, 2005, Moscow, in 5 vols. NIIZHB, 2005. Vol. 3. Section reports, section Concrete Technology, p. 228-234.

8. Abbas S., Nehdi M. L., Saleem M. A. Ultra-High Performance Concrete: Mechanical Performance, Durability, Sustainability and Implementation Challenges // International Journal of Concrete Structures and Materials. 2016. Vol. 10, No. 3. P. 271–295.

9. Gu C., Ye G., Sun W. Ultrahigh performance concrete-properties, applications and perspectives // Science China Technological Sciences. 2015. Vol. 58, Issue 4. P. 587-599.

10. Aitcin P.C. High-performance concrete, London: E&FN SPON, 1998. 591 p.

11. Мишина А.В. Исследование деформации использования высокопрочного сталифибробетона при

разгрузке // Academia. Архитектура и строительство. 2013. №3.

12. Мишина А.В., Безгодов И.М., Андрианов А.А. Прогнозирование предельных деформаций использования сверхвысокопрочного сталифибробетона // Вестник МГСУ. 2012. № 12.

13. Карпенко Н.И., Травуш В.И., Каприелов С.С., Мишина А.В., Андрианов А.А., Безгодов И.М. Исследования физико-механических и реологических свойств высокопрочного сталефибробетона // Academia. Архитектура и строительство. 2013. №1.

14. Карпенко Н.И., Травуш В.И. и другие. Методическое пособие «Статические неопределенные железобетонные конструкции. Диаграммные методы автоматизированного расчета и проектирования ». // Федеральное автономное учреждение «Федеральный центр стандартизации, стандартизации и оценки соответствия в строительстве». Москва, 2017.

15. Карпенко Н.И., Каприелов С.С., Петров А.Н., Безгодов И.М., Моисеенко Г.А., Степанов М.В., Чилин И.А. Исследование физико-механических и реологических свойств высокопрочных сталефибробетонов из самоуплотняющихся смесей // Фундаментальные, поисковые и прикладные исследования РААСН по научному обеспечению развития архитектуры, градостроительства и строительной отрасли Российской Федерации в 2017 году, т. 2. Москва, 2018. С. 237–246.

16. Каприелов С.С., Шейнфельд А.В., Кардумян Г.С. Новые модифицированные бетоны. Москва, ООО «Типография Парадиз». 2010. С. 258.

17. Каприелов С.С., Чилин И.А. Сверхвысокопрочный самоуплотняющийся фибробетон для монолитных конструкций // Строительные материалы, № 7. 2013. С. 28-30.

18. Каприелов С.С., Шейнфельд А.В., Кардумян Г.С., Дондуков В.Г. Модифицированные высокопрочные мелкозернистые бетоны с улучшенными деформативными характеристиками // Бетон и железобетон. 2006. № 2. С. 2-7.

19. Карпенко Н.И. Общие модели механики железобетона. Москва, Стройиздат, 1996.

20. Гвоздев А.А., Яшин А.В., Петрова К.В., Белобров И.К., Гузеев Е.А. Прочность, структурные изменения и деформации бетона. Москва, Стройиздат, 1978.

21. Малашкин Ю.Н., Безгодов И.М. Исследования длительной прочности и деформативности бетона при одно-, двух- и трехосном сжатии // Предельные состояния бетонных и железобетонных конструкций силовых сооружений. Материалы конференций и встреч по гидротехнике. Москва, 1987. С. 216-219.

22. Яшин А.В. Деформации бетона под продолжительным воздействием высоких напряжений и его длительное сопротивление сжатию // Особенности деформации бетона и железобетона и использование компьютеров для оценки их влияния на поведение конструкций. М .: Стройиздат, 1969. С. 38-76.

23. Степанов М.В., Моисеенко Г.А. Развитие экспериментального подхода к определению меры использования мелкозернистого высокопрочного бетона и сталифибробетона при рациональном содержании фибры // Строительство и реконструкция. 2018. № 3 (77). С. 98-104.

24. Степанов М.В., Моисеенко Г.А. Схема деформирования мелкозернистого высокопрочного бетона и сталефибробетона при сжатии. // Строительство и реконструкция. 2019. No3 (83). С. 11-21.

25. ГОСТ 24544-81 Бетон. Методы определения деформации усадки и использования.

Information about author:

Moiseenko Gennady A.
Research Institute of Building Physics RAABS, Moscow, Russia,
leadengineer.
E-mail: gecklock@yandex.ru

Информация об авторе:

Моисеенко Геннадий Анатольевич
Научно-исследовательский институт строительной физики РААБС, г. Москва, Россия,
главный инженер.
E-mail: gecklock@yandex.ru